RSC Advances

ROYAL SOCIETY OF CHEMISTRY

www.rsc.org/advances

Zwitterionic glutathione monoethyl ester as a new capping ligand for ultrasmall gold nanoparticles

Luiza L. Knittel†, Peter Schuck#, Christopher J. Ackerson§, Alioscka A. Sousa†,*

†Department of Biochemistry, Federal University of São Paulo, São Paulo 04044, Brazil.

National Institute of Biomedical Imaging and Bioengineering, National Institutes of Health, Bethesda 20892, USA.

§ Department of Chemistry, Colorado State University, Fort Collins 80521, USA.

Corresponding author: alioscka.sousa@unifesp.br

Abstract

The natural tripeptide glutathione has become a popular choice for passivating the surface of gold nanoparticles (NPs) intended for *in vivo* applications. Here we investigate a zwitterionic derivative of glutathione – glutathione monoethyl ester – as a new capping ligand for ultrasmall NPs. The new zwitterionic particles (AuGSH(zwt)) were colloidally stable in biological media and resistant against binding from serum proteins. AuGSH(zwt), but not glutathione-coated particles, could be successfully functionalized with strep-tag II for binding specifically to target streptactin in the presence of serum proteins. Taken together, these results place AuGSH(zwt) as a promising choice for attaining simultaneous *in vivo* renal clearance and targeted delivery via incorporation of functional peptides.

Gold nanoparticles (AuNPs) are a well-established platform for the development of new diagnostic and therapeutic tools in nanomedicine. Indeed, the size, shape and surface composition of AuNPs can be precisely tuned to regulate their bioresponses *in vivo*[1-2]. For example, to avoid potentially harmful long-term accumulation in the organism, AuNPs can be specially designed to be excreted in the urine[3-8]. This can be realized by engineering AuNPs of sufficiently small sizes and with stealth surface coatings to prevent nonspecific adsorption of plasma proteins. In this regard, ultrasmall (< 3 nm) AuNPs passivated with the natural tripeptide glutathione (GSH) have recently emerged as an effective nanoparticle system for attaining high rates of renal clearance[9-12].

Recently, we have investigated the behavior of ultrasmall GSH-coated particles (AuGSH) *in vitro*[13]. We observed a size threshold around 2 nm in core diameter below which AuGSH remained colloidally stable in biological media and resisted binding from serum proteins, in agreement with the efficient renal clearance reported for AuGSH *in vivo*. Surprisingly, however, particles of 2.5 nm in diameter were found to readily aggregate in biological media. We proposed that aggregation of the larger AuGSH was partially due to an interparticle attractive force generated by the increased number of COO^- groups and counterions (mainly Ca^{2+}, Mg^{2+}) at the particle surface.

In this work we sought to prepare a novel surface chemistry for ultrasmall AuNPs to overcome the partial, size-dependent stability of AuGSH in biological fluid as noted above. We hypothesized this could be achieved by using a zwitterionic ligand on the surface of the particles instead of negatively charged GSH. It might be expected that the net neutral charge of zwitterions will prevent the buildup of counterions at the particle surface as it happens for AuGSH. In addition, zwitterions have been currently investigated as nonfouling coatings for biomaterial surfaces and nanoparticles[5, 14-18]. The nonfouling properties of zwitterions are thought to derive from the formation of a strong, electrostatically induced hydration layer[18].

Our first choice for a zwitterionic ligand was the dipeptide CG, which corresponded to a truncated form of GSH (γ-ECG). The new zwitterionic AuNPs were prepared by ligand

exchange of ultrasmall (~ 2 nm) and highly uniform *p*-mercaptobenzoic acid-coated nanoparticles (AuMBA)[19-20] with CG. By following the strategy of ligand exchange, we expected the new AuNPs would maintain the size and uniformity of the parent AuMBA, as observed previously in the synthesis of AuGSH[13, 21]. In contrast, it is typically challenging to attain good control of particle size and uniformity from a direct synthesis approach whereby gold chloride is reduced with $NaBH_4$ in the presence of a new ligand[22-23].

Ligand exchange was performed over 3h with a 10:1 feed ratio of CG to *p*-mercaptobenzoic acid ligand. However, the reaction led to complete etching of AuMBA, as judged by the color of the solution changing from its original brown to clear. A screen of other candidate ligands revealed that the success of the reaction appears to depend on a combination of size and geometry of the incoming ligand (Fig. 1). We quantified the geometry of the ligands by measuring the cluster cone angle[24] of each ligand on a model $Au_{25}(SR)_{18}$ cluster, basing the initial model on a theoretical-experimental model of $Au_{25}(SG)_{18}$[25]. Cluster cone angle is a measurement that describes the relationship of the size of a ligand relative to a cluster centroid. Larger cluster cone angles are correlated with sterically more demanding ligands. We note that measurements of the cluster cone angles for these ligands are smaller on $Au_{144}(SR)_{60}$ clusters, but the trend will hold. We measured cone angles of 29.4°, 42.5°, 54.5°, and 62.0° for CG, tiopronin, GSH, and GSH monoethyl ester, respectively.

The cluster cone angle can account for differences in reactivity between ligands of similar mass. For instance, tiopronin and CG have similar molecular weight (163 vs 178 Da, respectively), but tiopronin has a notably different geometry, with a $–CH_3$ group in the vicinity of the –SH moiety. This geometric difference is reflected in the larger cone angle compared to CG. This larger cone angle, in turn, may limit the density of tiopronin ligands on the surface of the AuNPs. Conversely, small molecular weight compounds or molecules with small cone angles may facilitate etching of particles in addition to ligand exchange. We also note that some nanoparticle etching was observed in the presence of excess incoming ligand (independent of ligand identity) when extending the reaction time to 24h

(Fig. 1), suggesting that slow particle etching could occur in the cell cytoplasm as a result of the high intracellular GSH concentration[26].

Fig. 1 shows a derivative of GSH – glutathione monoethyl ester – which we found as a good choice for passivating the surface of ultrasmall AuNPs, since this molecule is zwitterionic and has similar size and cone angle as GSH. We also note that GSH monoethyl ester is a cell-permeable compound which is converted to GSH by intracellular esterases; thus, it has been proposed as a cellular GSH delivery agent[27]. The stability in plasma and biocompatibility of GSH monoethyl ester therefore constitute another positive feature of this molecule. We refer to particles coated with this new molecule as AuGSH(zwt) to underline the zwitterionic character of the ligand. We hereafter also refer to standard GSH-coated particles as AuGSH(neg) to emphasize the negative charge of GSH. The size and uniformity of AuGSH(zwt) were characterized by high-angle annular dark-field scanning transmission electron microscopy and analytical ultracentrifugation (Fig. 2).

We undertook a head-to-head comparison of the *in vitro* biointeractions of AuGSH(neg) and AuGSH(zwt). Importantly, these AuNPs had identical size distributions since they were both prepared by ligand exchange of AuMBA (Fig. 2c). Thus, the observed differences in the nanoparticles' bioresponses as reported below are solely due to the chemical nature of the capping ligand without any interference from size variations. We first checked whether the structural integrity of AuGSH(neg) and AuGSH(zwt) would be compromised by incubation in cell culture medium. This could occur by ligand exchange of the AuNPs with cysteine (and possibly with other amino acids as well via their terminal amino groups). For this experiment, we incubated AuGSH(neg) and AuGSH(zwt) in pure cell culture medium for 7 days, transferred the particles from medium to PBS by centrifuge filtration, and recorded absorbance spectra to verify if any particle degradation had taken place. No alterations in the UV-vis spectra of the nanoparticles were observed, suggesting their structural integrity was preserved (data not shown). This can be understood considering the relatively small concentration of cysteine in culture medium (~ 0.2 mM), in contrast with the high intracellular GSH concentrations (up to 10 mM) as already noted.

Next, UV-visible spectroscopy was utilized to assess the colloidal stability of AuGSH(neg) and AuGSH(zwt) in pure cell culture medium. We first recall that the absorbance spectra of 2 nm-diameter AuNPs display only a shoulder in the range of 500 nm, instead of the characteristic surface plasmon resonance peak of larger AuNPs. Nevertheless, aggregation of these ultrasmall particles can be observed by UV-vis spectroscopy as a significant increase in absorbance in the range of 500 nm and beyond. While no significant changes occurred in the absorbance spectrum of AuGSH(zwt) up to 24h in culture medium, the spectrum of AuGSH(neg) indicated the presence of large aggregates after only a 2h incubation period in medium (Fig. 3a,b). Because of the limited sensitivity of UV-vis spectroscopy in detecting small particle agglomerates, we further assessed the presumed colloidal stability of AuGSH(zwt) by analytical ultracentrifugation (AUC)[13]. We estimate that AUC would be sensitive enough to detect "aggregates" as small as nanoparticle dimers. The similar sedimentation coefficient distributions of AuGSH(zwt) shown in Fig. 3c confirmed the particles' stability in cell culture medium.

Next, we utilized AUC to characterize AuGSH(neg) and AuGSH(zwt) in 10% FBS-supplemented PBS. AuGSH(neg) particles aggregated in FBS as indicated by a 60% reduction in area under their sedimentation coefficient distributions relative to control (Fig. 4a). As previously reported, the aggregation of AuGSH(neg) in FBS is not caused by serum proteins; instead, it appears to be mainly driven by divalent cations (Ca^{2+}, Mg^{2+}) present in serum[13]. While approximately 40% of AuGSH(neg) remained dispersed in solution, the particles sedimented slower when compared to particles in PBS. This observation suggests the binding of serum proteins onto AuGSH(neg), which increases the hydrodynamic friction and lowers the overall density of the liganded particles thus reducing their sedimentation velocity. In contrast, the sedimentation coefficient distributions for AuGSH(zwt) in 10% FBS and PBS control were virtually identical to each other, therefore indicating lack of both aggregation and binding of serum proteins (Fig. 4b). Notably, we also carried out a more rigorous test by first incubating AuGSH(zwt) in pure FBS for 24h before finally diluting to 10% FBS-PBS prior to loading into the

ultracentrifuge. Again, the results revealed no evidence of aggregation or significant serum protein interactions with AuGSH(zwt) (Fig. 4c).

As another comparison, we investigated the intracellular uptake of the AuNPs by RAW 264.7 macrophages. The amount of internalized nanoparticles was quantified by inductively coupled plasma mass spectrometry (ICP-MS). The results showed a significantly lower level of uptake of AuGSH(zwt) compared to AuGSH(neg), consistent with the expectation that AuGSH(zwt) should interact minimally (if at all) with the plasma membrane (Fig. S1).

The ultrasmall size, uniformity, colloidal stability and stealth character of AuGSH(zwt) as discussed so far would place this nanoparticle as a potential candidate for *in vivo* applications requiring renal clearance. Interestingly, renal-clearable ultrasmall AuNPs have also been shown to display long tumor retention characteristics[9, 12]. Efficient cancer therapy, however, might require an "active" targeting mechanism by which functional ligands concentrate the nanoparticles preferentially in the tumor environment [28-29]. It is clear that for this targeting approach to work in practice the functional moiety must remain exposed on the particle surface, i.e., it must not be shielded by a layer of adsorbed proteins[30-35].

We thus tested whether a functional peptide, strep-tag II (WSHPQFEK), attached to AuGSH(zwt) would bind its target protein, streptactin, in the presence of serum proteins. It is known that strep-tag II binds streptactin with a dissociation constant around 1 μM[36], which is within the relevant range of high nanomolar to low micromolar affinity[37] (on the other hand, high-affinity interactions between ligands and tumor cell receptors might prove counterproductive *in vivo* due to the binding-site barrier phenomenon[37-38]). The functional peptide was synthesized as ECGGGWSHPQFEK, where the Cys provided the –SH group for anchoring onto the AuNP surface, the N-terminal Glu was added to increase the cluster cone angle, and the three Gly were added to keep the binding portion of the extended peptide sufficiently separated from the particle surface. The successful

functionalization of AuGSH(neg) and AuGSH(zwt) with strep-tag II was confirmed as described in Fig. S2.

Fig. 5a illustrates the binding experiment in a schematic fashion. Functional AuGSH(neg) and AuGSH(zwt) were diluted in FBS and next added to an equal volume of streptactin-coated sepharose beads. After settling of the beads, UV-vis spectroscopy was used to detect the presence of AuNPs in the supernatant. As Fig. 5b,c shows, strep-tagged AuGSH(zwt) bound streptactin leading to a supernatant phase depleted of nanoparticles, whereas strep-tagged AuGSH(neg) interacted preferentially with serum proteins thus remaining mostly in the supernatant.

To gain further insights into the particles' interactions in serum, we repeated the above experiments now with ECGK-biotin attached on their surface. Relative to strep-tagged AuGSH(neg), the new biotinylated AuGSH(neg) particles interacted more efficiently with streptactin-coated sepharose beads in the presence of FBS (Fig. S3; compare with Fig. 5b). This finding was expected given the very high-affinity (< pM) interaction of biotin with streptactin. However, still a significant amount of AuGSH(neg) remained in the supernatant due to nonspecific binding with serum proteins. Finally, biotinylated AuGSH(zwt) was found to bind the streptactin beads completely leaving a supernatant phase free of nanoparticles (Fig. S3). This result is consistent with the stealth nature of AuGSH(zwt) and the strong interaction between biotin and streptactin.

In summary, we have investigated a zwitterionic derivative of glutathione – glutathione monoethyl ester – as a new ligand for passivating the surface of ultrasmall AuNPs. The high cluster cone angle of this ligand enabled it to be used in ligand exchange reactions with AuMBA particles, therefore yielding new AuGSH(zwt) with the same ultrasmall size and uniformity of the parent AuMBA. AuGSH(zwt) was found to be resistant against aggregation and binding from serum proteins within the experimental conditions applied. We finally established that AuGSH(zwt) functionalized with the strep-tag II peptide could bind the target protein streptactin in the presence of FBS, whereas functionalized AuGSH(neg) did not bind streptactin efficiently due to a 'shielding effect' from the

interacting serum proteins. Collectively, these results raise the possibility that AuGSH(zwt) might be retained in the tumor environment *in vivo* by incorporation of functional peptides, while allowing for efficient renal clearance of off-tumor circulating particles.

ASSOCIATED CONTENT

Electronic supplementary information (ESI) available.

CORRESPONDING AUTHOR

* Corresponding author: alioscka.sousa@unifesp.br

ACKNOWLEDGMENT

We would like to acknowledge Prof. M.L.V. Oliva for providing access to instrumentation, and Dr. M.A. Aronova and Dr. R.D. Leapman for images of gold nanoparticles. We acknowledge the Spectroscopy and Calorimetry facility at Brazilian Biosciences National Laboratory (LNBio/CNPEM) for their support with the analytical ultracentrifuge. This work was supported by the São Paulo Research Foundation (FAPESP: 2013/18481-5) and by the Brazilian National Council for Scientific and Technological Development (CNPq: 476784/2013-1). CJA acknowledges NSF CHE 1455099.

REFERENCES

1. S. Rana, A. Bajaj, R. Mout and V. M. Rotello, *Adv. Drug Deliv. Rev.*, 2012, **64**, 200-216.
2. A. Albanese, P. S. Tang and W. C. W. Chan, *Annu. Rev. Biomed. Eng.* , 2012, **14**, 1–16.
3. X. D. Zhang, J. Yang, S. S. Song, W. Long, J. Chen, X. Shen, H. Wang, Y. M. Sun, P .X. Liu and S. Fan, *Int. J. Nanomed.*, 2014, **9**, 2069–2072.
4. C. Zhou, M. Long, Y. Qin, X. Sun and J. Zheng, *Angew. Chem. Int. Ed.*, 2011, **50**, 3168 –3172.
5. K. P. García, K. Zarschler, L. Barbaro, J. A. Barreto, W. O'Malley, L. Spiccia, H. Stephan and B. Graham, *Small*, 2014, **10**, 2516–2529.
6. A. Leifert, Y. Pan-Bartnek, U. Simon and W. Jahnen-Dechent, *Nanoscale*, 2013, **5**, 6224–6242.
7. O. A. Wong, R. J. Hansen, T. W. Ni, C. L. Heinecke, W. S. Compel, D. L. Gustafson and C. J. Ackerson, *Nanoscale*, 2013, **5**, 10525–10533.
8. M. Yu and J. Zheng, *ACS Nano*, 2015, **9**, 6655–6674.
9. J. Liu, M. Yu, C. Zhou, S. Yang, X. Ning and J. Zheng, *J. Am. Chem. Soc.*, 2013, **135**, 4978-4981.
10. C. A. Simpson, K. J. Salleng, D. E. Cliffel and D. L. Feldheim, *Nanomedicine: Nanotech. Biol. Med.*, 2013, **9**, 257-263.

11. X. D. Zhang, J. Chen, Z. Luo, D. Wu, X. Shen, S.S. Song, Y.M. Sun, P.X. Liu, J. Zhao, S. Huo, S. Fan, F. Fan, X.J. Liang and J. Xie, *Adv. Healthcare Mat.*, 2013, **3**, 133–141.
12. X. D. Zhang, Z. Luo, J. Chen, S. Song, X. Yuan, X. Shen, H. Wang, Y. Sun, K. Gao, L. Zhang, S. Fan, D. T. Leong, M. Guo and J. Xie, *Scientific Reports*, 2015, **5**.
13. A. A. Sousa, S. A. Hassan, L. L. Knittel, A. Balbo, M. A. Aronova, P. H. Brown, P. Schuck and R. D. Leapman, *Nanoscale*, 2016, **8**, 6577-6588.
14. D. F. Moyano, K. Saha, G. Prakash, B. Yan, H. Kong, M. Yazdani and V. M. Rotello, *ACS Nano*, 2014, **8**, 6748–6755.
15. W. Yang, L. Zhang, S. Wang, A. D. White and S. Jiang, *Biomaterials*, 2009, **30**, 5617-5621.
16. J. E. Rosen and F. X. Gu, *Langmuir*, 2011, **27**, 10507–10513.
17. J. B. Schlenoff, *Langmuir*, 2014, **30**, 9625–9636.
18. S. Jiang and Z. Cao, *Adv. Mater.*, 2010, **22**, 920–932.
19. C. L. Heinecke and C. J. Ackerson, *Methods Mol. Biol.*, 2013, **950**, 293-311.
20. C. J. Ackerson, P. D. Jadzinsky, J. Z. Sexton, D. A. Bushnell and R. D. Kornberg, *Bioconj. Chem.*, 2010, **21**, 214-218.
21. A. A. Sousa, J. T. Morgan, P. H. Brown, A. Adams, M. P. S. Jayasekara, G. Zhang, C. J. Ackerson, M. J. Kruhlak and R. D. Leapman, *Small*, 2012, **8**, 2277–2286.
22. C. J. Ackerson, P. D. Jadzinsky and R. D. Kornberg, *J. Am. Chem. Soc.*, 2005, **127**, 6550–6551.
23. O. A. Wong, W. S. Compel and C. J. Ackerson, *ACS Combinatorial Sci.*, 2015, **17**, 11-18.
24. D. M. P. Mingos, *Inorg. Chem.*, 1982, **21**, 464–466.
25. V. Rojas-Cervellera, C. Rovira and J. Akola, *J. Phys. Chem. Lett.* , 2015, **6**, 3859-3865.
26. R. Hong, G. Han, J. M. Fernández, B. J. Kim, N. S. Forbes and V. M. Rotello, *J. Am. Chem. Soc.*, 2006, **128**, 1078–1079.
27. M. E. Anderson, F. Powrie, R. N. Puri and A. Meister, *Archives Biochem. Biophysics*, 1985, **239**, 538–548.
28. L. Yao, J. Daniels, A. Moshnikova, S. Kuznetsov, A. Ahmed, D. M. Engelman, Y. K. Reshetnyak and O. A. Andreev, *Proc. Nat. Acad. Sci. USA*, 2013, **110**, 465-470.
29. D. Simberg, T. Duza, J. H. Park, M. Essler, J. Pilch, L. Zhang, A. M. Derfus, M. Yang, R. M. Hoffmang, S. Bhatia, M. J. Sailor and E. Ruoslahti, *Proc. Nat. Acad. Sci. USA*, 2007, **104**, 932–936
30. A. Salvati, A. S. Pitek, M. P. Monopoli, K. Prapainop, F. B. Bombelli, D. R. Hristov, P. M. Kelly, C. Åberg, E. Mahon and K. A. Dawson, *Nat. Nanotech.*, 2013, **8**, 137–143.
31. J. Lazarovits, Y. Y. Chen, E. A. Sykes and W. C. W. Chan, *Chem. Commun.*, 2015, **51**, 2756-2767.
32. B. S. Varnamkhasti, H. Hosseinzadeh, M. Azhdarzadeh, S. Y. Vafaei, M. Esfandyari-Manesh, Z. H. Mirzaie, M. Amini, S. N. Ostad, F. Atyabi and R. Dinarvand, *Int. J. Pharm.*, 2015, **494**, 430–444.
33. D. Maiolo, P. D. Pino, P. Metrangolo, W. J. Parak and F. B. Bombelli, *Nanomedicine*, 2015, **10**, 3231-3247.
34. V. Mirshafiee, M. Mahmoudi, K. Lou, J. Cheng and M. L. Kraft, *Chem. Commun.*, 2013, **49**, 2557-2559.
35. R. D. Vinluan, M. Yu, M. Gannaway, J. Sullins, J. Xu and J. Zheng, *Bioconj. Chem.*, 2015, **26**, 2435-2441.
36. A. Skerra and T. G. M. Schmidt, *Biomol. Eng.*, 1999, **16**, 79–86.
37. E. Ruoslahti, S. N. Bhatia and M. J. Sailor, *J. Cell Biol.*, 2010, **188**, 759-768
38. W. van Osdol, K. Fujimori and J. N. Weinstein, *Cancer Res*, 1991, **51**, 4776-4784.

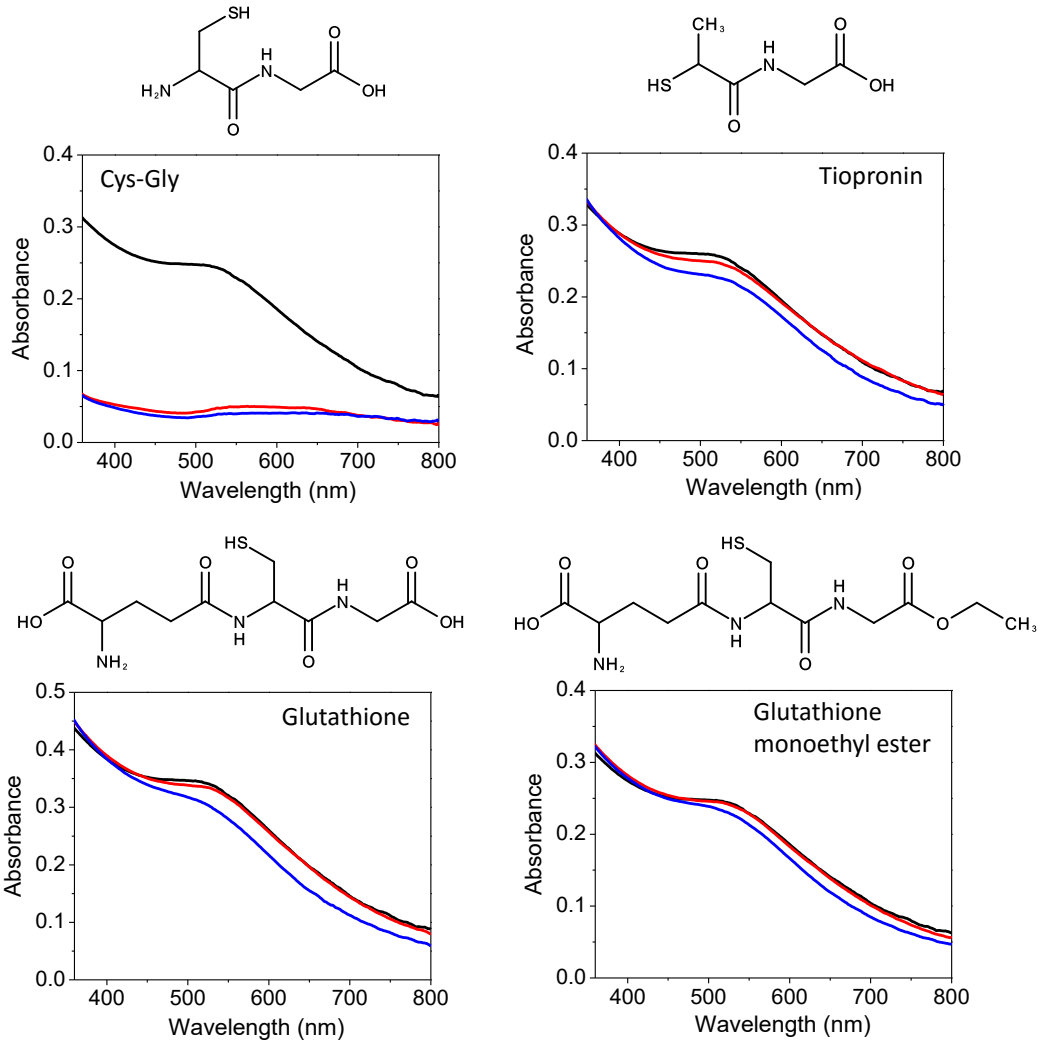

Figure 1. Nanoparticle etching during ligand exchange assessed by UV-vis spectroscopy. Ligand exchange with CG leads to rapid degradation of nanoparticles. Etching is not observed for other selected ligands due to their larger cluster cone angles (but minor nanoparticle etching is observed when extending the reaction time to 24h). Black traces, UV-vis spectra of AuNPs in PBS; red traces, after 3h ligand exchange; blue traces, after 24h ligand exchange

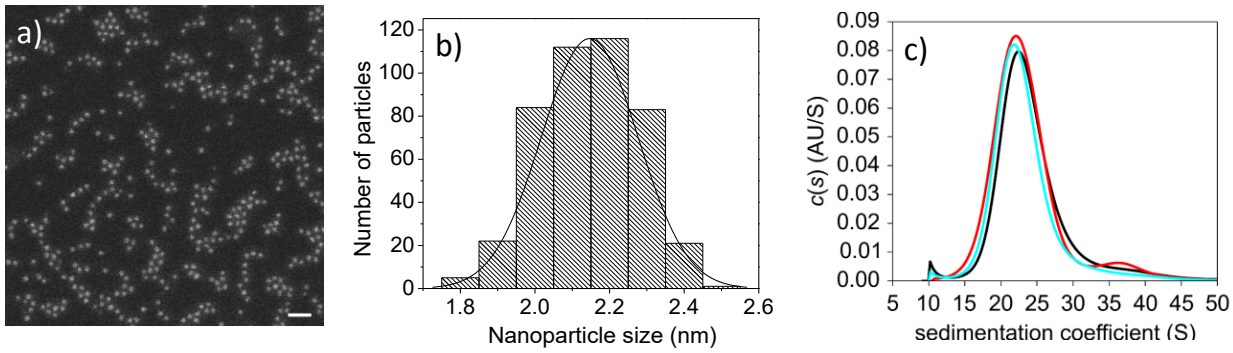

Figure 2. Characterization of AuGSH(zwt) size and uniformity. (a) Dark-field scanning transmission electron microscopy (STEM) image of AuGSH(zwt) illustrating the particles' high uniformity. Scale bar, 10 nm. (b) Histogram of STEM measurements of nanoparticle diameter. Average core diameter = 2.1 ± 0.1 nm. (c) Analytical ultracentrifugation analysis of AuMBA (black), AuGSH(neg) (red) and AuGSH(zwt) (cyan). Coinciding sedimentation coefficient distributions show that AuGSH(neg) and AuGSH(zwt) have the same uniformity and similar size and density as the parent AuMBA nanoparticles.

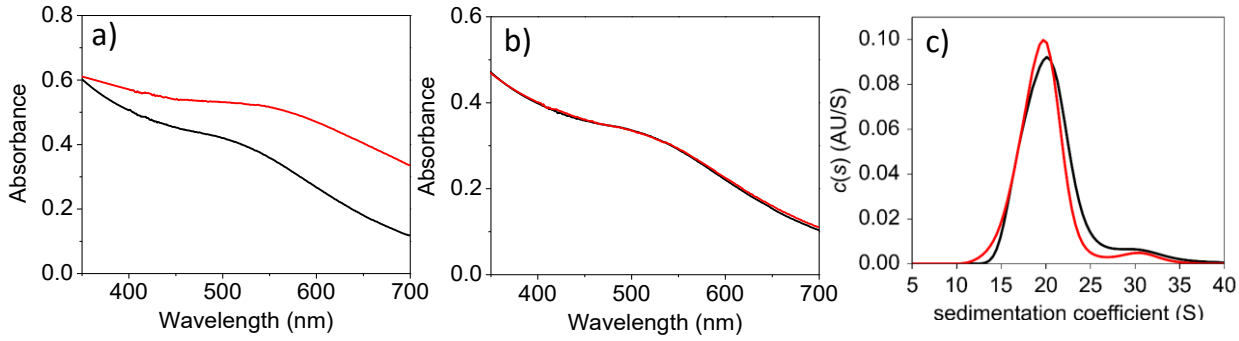

Figure 3. Aggregation of AuGSH(neg) and AuGSH(zwt) in pure cell culture medium. UV-vis spectra of (a) AuGSH(neg) and (b) AuGSH(zwt) in PBS (black traces) and pure cell culture medium (red traces). Only AuGSH(neg) is seen to undergo significant aggregation in culture medium. (c) A highly sensitive analytical ultracentrifugation analysis confirmed the colloidal stability of AuGSH(zwt) in culture medium (black: PBS; red: medium).

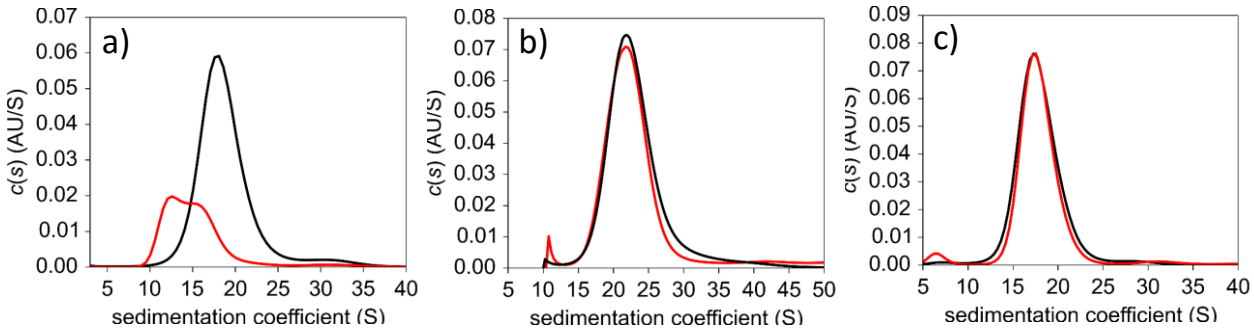

Figure 4. Analytical ultracentrifugation analysis of AuGSH(neg) and AuGSH(zwt) in the presence of FBS. (a) Approximately 60% of AuGSH(neg) particles form sufficiently dense aggregates in FBS that sediment beyond 40 S. Remaining AuGSH(neg) particles in solution (~ 40%) are bound with serum proteins. (b) Coinciding sedimentation coefficient distributions of AuGSH(zwt) in 10% FBS and PBS indicate lack of both aggregation and serum protein interactions. (c) Similar to b), but with pre-incubation of AuGSH(zwt) in 100% FBS for 24h prior to loading into the ultracentrifuge at 10% FBS. Black traces, AuNPs in PBS; red, AuNPs in 10% FBS-PBS.

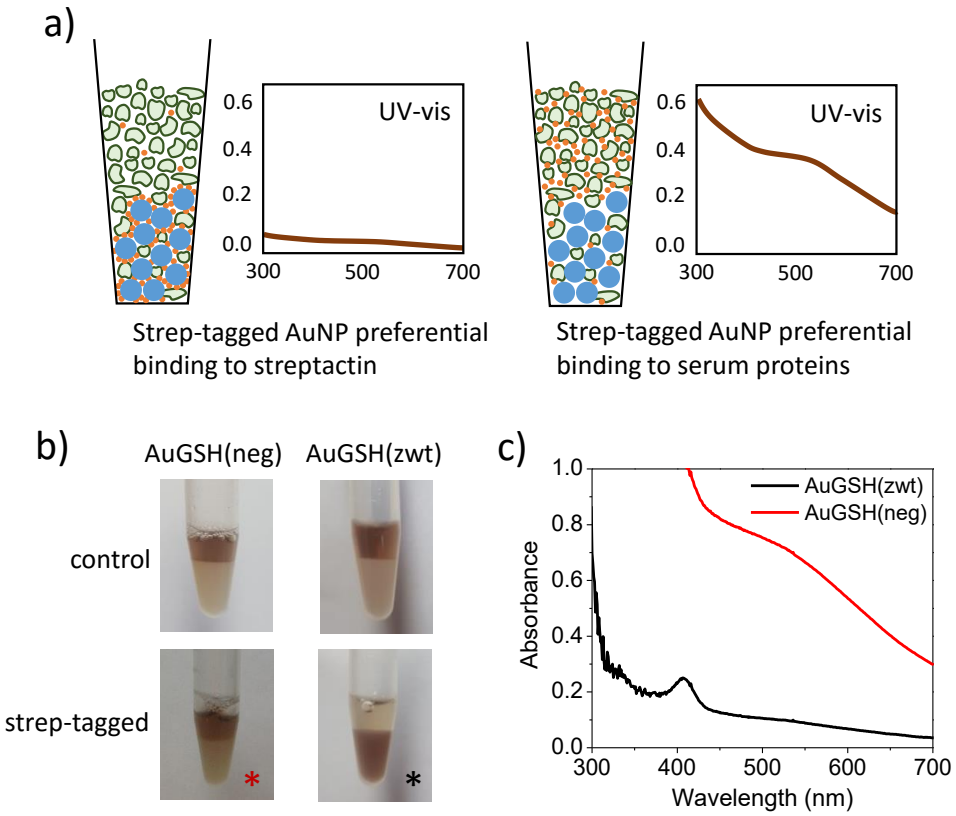

Figure 5. Binding of strep-tagged AuNPs to streptactin in the presence of serum proteins. (a) Schematic illustration of pull-down-type binding assay (drawing is not to scale). AuNPs functionalized with strep-tag II (orange) are pre-incubated in pure FBS (serum proteins in green). Next, streptactin-coated sepharose beads (blue) are added to the nanoparticle-serum mixture and left to settle down. UV-vis spectroscopy is used to detect the presence of AuNPs in the supernatant. AuNPs settle down with the beads when they preferentially bind streptactin over serum proteins. (b) Pictures of solutions of non-functionalized (control) and strep-tagged nanoparticles with FBS and streptactin-coated beads. Nanoparticle-rich phase appears with dark brown color. Only strep-tagged AuGSH(zwt) binds streptactin preferentially over the serum proteins leading to a clearer supernatant phase. (c) UV-vis spectra of supernatant of solutions marked with an asterisk in b). The peak at 400 nm for AuGSH(zwt) corresponds to FBS components.

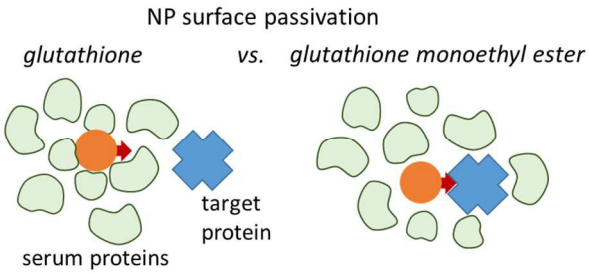

Ultrasmall gold nanoparticles coated with a zwitterionic derivative of glutathione are shown to be stable against aggregation and nonspecific binding from serum proteins.